



Friction stir vibration brazing (FSVB): an improved version of friction stir brazing

Mahmoud Abbasi¹ · Behrouz Bagheri² · Farzaneh Sharifi³ · Amin Abdollahzadeh⁴

Received: 31 October 2020 / Accepted: 11 August 2021 / Published online: 26 August 2021
© International Institute of Welding 2021

Abstract

Friction stir vibration brazing (FSVB) by application of mechanical vibration was introduced in this investigation. In the current research, the adjoining samples are vibrated normally to the brazing line while FSB is performed. Low carbon steel sheets are joined together using FSB and FSVB while SiC nanoparticles are also incorporated in the joint. The microstructure and mechanical behavior of the joints developed under different conditions are analyzed. %67wt Sn-%33wt Pb alloy is used as braze metal. The results show that the strength of the friction stir vibration brazed specimens is higher than that of the friction stir brazed specimens. The vibration of adjoining specimens, during FSVB, enhances the eutectic reaction of the melt braze metal between the adjoining specimens and the melt fills the space between adjoining specimens thoroughly. By introducing vibration during the FSB process, both strain rate and temperature which have fundamental effects on the characteristics of the joints, increase. The results indicate that the strength and the hardness of FSVB-ed samples increase and the grain size decreases as vibration frequency increases from 30 to 60 Hz. In addition, the thickness of IMCs in the joint interface decreased to around 0.7 μm as the vibration frequency increased.

Keywords Friction stir brazing · Friction stir vibration brazing · Reinforcing particles · Mechanical properties · Microstructure

1 Introduction

Brazing is a joining process used to join different types of metals together by molten brazing metal. The tin–lead (Sn–Pb) alloys have been the conventional brazing metals or fillers applied for brazing in various industries such as

the electronic assemblies, typically package-to-board assemblies. This is because of their accessibility, low melting temperature, low cost, excellent wettability on most of the substrate materials, and ability to prevent the transformation of β -Sn to α -Sn at a temperature below 13 °C [1, 2]. However, the utilization of these Sn–Pb brazing metals has been limited because of the inherent toxicity of lead and much has been performed to develop lead-free fillers. The addition of nanosized reinforcements to the joint region refines the braze matrix microstructure and reduces the formation of interfacial intermetallic compounds (IMCs) through the particle adsorption mechanism and improves the mechanical properties because of the particle dispersion strengthening mechanism. However, it has been shown that the performance of a composite lead-free joint remarkably depends on the interaction between the added reinforcement with both the lead-free filler and the base materials [3, 4].

Brazing, as a joining technique, involves some steps: placing of brazing metal between adjoining specimens, heating the specimens, melting of brazing metal, filling of molten filler metal between the joining specimens, and then solidification [5, 6]. An attractive characteristic of this process

Recommended for publication by Commission XVII - Brazing, Soldering and Diffusion Bonding

✉ Behrouz Bagheri
b.bagheri@aut.ac.ir

Mahmoud Abbasi
m.abbasi@kashanu.ac.ir

¹ Faculty of Engineering, University of Kashan, Kashan, Iran

² Department of Mining and Metallurgy, Amirkabir University of Technology, Tehran, Iran

³ School of Mechanical and Materials Engineering, Washington State University, Pullman, WA, USA

⁴ Department of Materials Science and Engineering, Faculty of Engineering, Shahid Chamran University of Ahvaz, Ahvaz, Iran

is that a permanent joint is obtained without the melting of base workpieces. Friction stir brazing (FSB) was initially developed by Zhang et al. in 2011 [7].

In FSB, brazing metal between two adjoining plates is melted when a rotating tool is applied on the surface of the joining specimen. The friction between the rotating shoulder and joining specimen produces the heat required for the melting of brazing metal. Unlike the conventional friction stir welding (FSW) process where joining is obtained only by a plastic flow driven by a rotating pin, joining in FSB is obtained fundamentally by metallurgical reaction with the aid of mechanical influence of large rotating shoulder [8]. During the FSB process, a pinless tool is applied to remove the keyhole, hook, and severe wear of pin tip by strong base metal. A preplaced braze/solder is utilized to eliminate oxide film by eutectic reaction between braze and base metal. Subsequently, oxide film fragments are expelled with the formed eutectic liquid phase. Finally, bonded region width up to shoulder diameter extends [9, 10]. Using brazing metal with a lower solidus temperature is an effective way of reducing the residual stress in the joint.

Particles with a low coefficient of thermal expansion (CTE), such as Al_2O_3 , Si_3N_4 , and SiO_2 , have been added to the filler metal matrix to improve the strength and mechanical properties of the joint. Yang et al. [11] added Al_2O_3 into the conventional filler and found that interfacial layer growth depends on the volume fraction of the Al_2O_3 particles. The strength of the joint, as the void volume fraction of the Al_2O_3 exceeded 10%, reduced dramatically due to the very low fluidity of the liquid brazing metal. Chuang et al. [12] applied Al_2O_3 nanoparticles to reinforce Sn–Ag–Cu filler alloy. The mechanical properties decreased as the content of Al_2O_3 was merely over 1.5 wt%, which is far from sufficient to decrease the CTE of the brazing metal. For solid-state bonded joints of dissimilar metals, the joint strength is determined by two predominant factors, namely the intimate contact between the joining interfaces and the interfacial microstructure, particularly the formation of intermetallic compounds (IMCs). The microstructure and mechanical properties of the lap joint manufactured by FSB between Ti-6Al-4 V and 321 stainless steel were investigated by Javadi et al. [13]. They used Ag–Cu braze alloy. They reported some intermetallic phases such as TiCu, Ti_2Cu , and Fe–Cu–Ti in joint and indicated that the shear strength of joint decreased and microhardness increased as intermetallic layer thickness increased.

By application of the FSB process and zinc foil as filler or brazing metal, Zhang et al. [7] manufactured Al/steel layered composite. It was reported that most Zn was extruded and several Al–Fe intermetallic compounds with a little Zn were formed in the interfacial region. The FSB process was used by Huang et al. [14] to join 6061 Al to H62 brass with the application of zinc foil as a brazing metal. They analyzed the interfacial microstructure evolution under different joining speeds.

In addition, the effect of zinc foil on fracture performance and diffusion generations on both aluminum and brass sides was studied. It was concluded that the variation of traveling speed influences the thickness of the interlayer and also the cooling rate.

Up to now, many types of research have been carried out to improve FSB to develop the microstructure and mechanical properties of the joints [15, 16]. Ultrasonic brazing originated in Germany, and the first patent for ultrasonic brazing was invented in 1939. By the 1970s, ultrasonic brazing had been used in joining various metals, ceramics, and composite materials [17]. Wei et al. [15] studied the effect of ultrasonic vibration during the brazing of composite joints of sapphire. It was concluded that the dramatic dissolution between the aluminum alloy matrix in the composite interlayer occurred during the brazing process, and the maximum shear strength of ~155 MPa was achieved. Huang et al. [18] applied ultrasonic-assisted induction brazing (UAIB) to join the diamond onto the 1045 steel. A brazed filler surface with fewer slags and also a bond zone with fewer and smaller cracks were achieved compared to the conventional induction brazing. Xu et al. [19] applied the ultrasonic-assisted brazing method to analyze the microstructure and mechanical properties of the joint formed between 30 vol.% Si_3N_4 /6061Al composites using a Zn–Al alloy as filler metal. They indicated that by application of ultrasonic action, the surface oxide layer between the filler metal and composites broke and a composite bond with uniform distribution of the reinforcements was formed. They also found that the proportion of Si_3N_4 particles and the Al atomic percentage in the bond layer enhanced as the ultrasonic action duration and the brazing temperature increased. The mechanical and microstructure behaviors of the bonded zone between Ti-6Al-4 V alloy and ZrO_2 ceramic with Al-5wt%Si brazing filler during the ultrasonic-assisted brazing process were examined by Zhang et al. [20]. It was found that ultrasonic had an important role in the formation of Si segregation regions near the interface of Ti-6Al-4 V and in the center of the joint. Additionally, they reported that the shear strength of the joint increased as ultrasonic was applied during the brazing process.

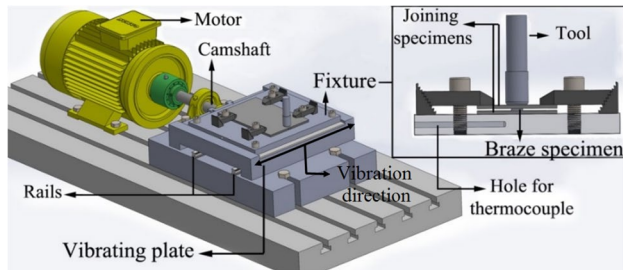
In the current investigation, a modified version of the FSB process, called “friction stir vibration brazing” (FSVB), is presented. The microstructures and mechanical properties of joints made by FSB and FSVB are compared. Additionally, the influence of the addition of SiC nanoparticles on different properties of the joints developed between low carbon steels by FSB and FSVB processes is studied.

2 Materials and methods

In this study, a low carbon steel plate with a thickness of 3 mm was used as the base material. The chemical composition of the studied material is presented in Table 1. The plate

Table 1 Chemical composition of the adjoining steel plates (% wt.)

C	Si	Mn	Cr	Mo	Ni	Al	Cu	P	S	Fe
0.1	0.3	0.6	0.45	0.02	0.25	0.03	0.2	0.03	0.005	Balance

**Fig. 1** Schematic design of machine applied for FSVB and detailed scheme of fixture used for FSB and FSVB

was cut into rectangle specimens with 210-mm length and 210-mm width. Abrasive paper (grit size 400) was applied to polish the joining surfaces before the brazing, and acetone was used to remove the grindings and the impurities. A sheet of Sn–Pb alloy (%67wt Sn–%33wt Pb) with a thickness of 2 mm and a melting point of about 187 °C was used as filler (braze) metal. Rectangle specimens with 210-mm length and 30-mm width were prepared from the filler sheet. The filler specimen was positioned between adjoining specimens and brazing was carried out by application of a milling machine.

For FSVB, the joining specimens, which contained filler metal in between, were fixed on the fixture, and the fixture was placed on a vibrating plate. The plate moves on two guide rails base on the camshaft mechanism. The motor shaft rotation is transformed into a linear and reciprocating movement of the vibrating plate by a camshaft. The schematic design of the machine manufactured for carrying out FSVB is displayed in Fig. 1. Based on the camshaft design, the vibration amplitude is 0.5 mm and the vibration frequency is adjusted by a driver. The machine is installed on a milling machine. Various trials with different values for affecting parameters of FSB were done and the optimum values for FSB parameters were achieved (Table 2). For non-optimum values of parameters, the appearance of joints was unfair and the strength was very low. Optimum values were also applied for FSVB. In Table 2, the conditions for all FSB and FSVB processes, analyzed in the current research, are presented.

FSVB differs remarkably from brazing assisted by ultrasonic vibration. During the latter method, the tool is vibrated by ultrasound waves while the vibration amplitude is around 10–50 μm and vibration frequency is in the range of 20–50 kHz. In FSVB, the joining specimens are vibrated using a vibrating machine while the vibration amplitude is about 0.1–0.5 mm and vibration frequency is in the range

Table 2 Brazing conditions for FSB and FSVB

	Rotational speed (rpm)	Traverse speed (mm/min)	Vibration frequency (Hz)
FSB	1100	75	-
FSVB	1100	75	25
FSVB	1100	75	30
FSVB	1100	75	45
FSVB	1100	75	60

of 20–100 Hz. Therefore, vibration frequency for brazing assisted by ultrasonic vibration is higher than that for FSVB, but vibration amplitude for FSVB is higher than that for the ultrasonic-assisted brazing process.

The effect of the incorporation of SiC particles into the braze matrix microstructure was also studied in this research. SiC particles with a nominal diameter of 10 nm were used as reinforcing particles. The weight of powders for all samples was the same (0.04 g). For all brazing conditions, the particles were distributed homogeneously on the filler metal sheet prior to brazing. The tool consisted of a shoulder from M2 steel with a hardness of 65 HRC. The geometry for the tool is presented in Fig. 2.

Transverse sections of brazed specimens were prepared and mechanically polished based on the standard metallographic procedure (ASTM E3-11) to reveal the microstructure and analyze the powder distribution. The mechanical strength of the joints was investigated by tensile shear tests. The tensile shear tests according to ASTM D1002-10 were carried out to measure the shear strength of joints. The shear test specimens were prepared by application of wire cut (electro-discharge machining). The schematic design of a shear test specimen is displayed in Fig. 3. The specimens were loaded at a rate of 1 mm/min on a WDW-1000 mechanical tensile tester. For each brazing condition, 3 specimens were prepared and the force versus displacement data was measured for each specimen.

The microstructural study was carried out by using scanning electron microscopy (SEM), light optical microscopy (LOM), and transmission electron microscopy (TEM). A hardness measurement was performed on the transverse section of brazed specimens with the help of a Vickers microhardness testing machine. Force was 25 gr and dwell time was 10 s. Five replicates were determined for each brazing condition. The distance between test points was higher than 6 times the diameter

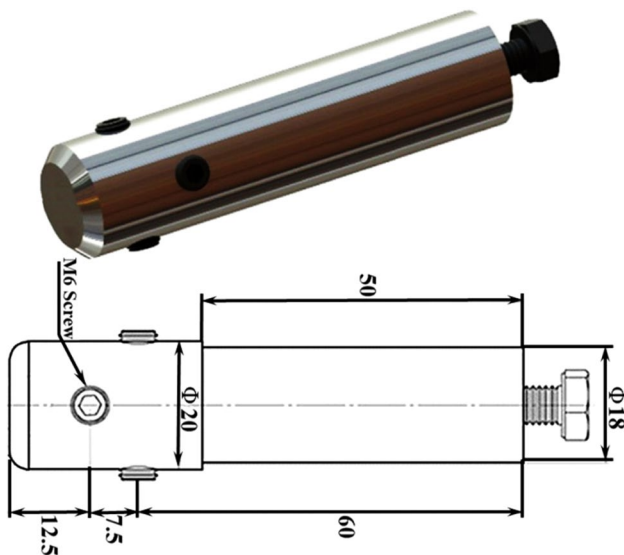


Fig. 2 Schematic design of the tool applied for FSB and FSVB (all dimensions are in mm)

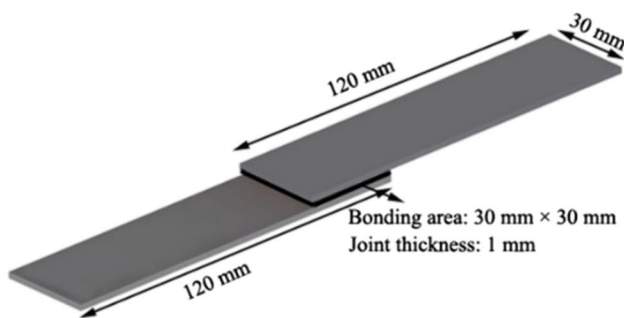


Fig. 3 Schematic design of shear test specimens

of indentations. To measure the temperature changes of the fixture during various brazing conditions, a K-type thermocouple was utilized. A hole was cut in the fixture and the thermocouple was positioned in it (Fig. 1). The thermocouple records the temperature of a fixed point of fixture beneath the brazing line.

The total area of the interfacial intermetallic compound (IMC) layer and its length were calculated utilizing image analysis software (Image J, NIH software). In this examination, the IMC layer thickness was measured using the following relationship:

$$h = A/L \quad (1)$$

where A is the area of the IMCs layer and L is the length. The average IMC layer thickness was achieved from the SEM images taken at ten different spots.

3 Results and discussion

3.1 Influence of vibration during FSB

Cross-section macrostructures of joints for different conditions, namely FSB and FSVB (with a vibration frequency of 25 Hz), are presented in Fig. 4. While coherent interfaces are observed for FSVB-ed specimens, the interfaces for FSB-ed specimen are incoherent and porosities are observed in the joint region. The friction between the rotating shoulder and the joining specimen generates heat which melts the filler. Brazing occurs as filler metal is solidified and IMCs form in the microstructure during solidification. Porosities and IMC layers are observed for FSB-ed specimens, but in all FSVB-ed specimens, the joints are without porosities and continuous IMC layers are observed. This can be because of the influence of vibration in FSVB. During FSB, the oxide film of base metal and interlayer rupture, and fresh metal surfaces contact with each other and the diffusion of elements occurs. The presence of vibration during FSB improves the friction between the shoulder and joining metal surfaces and as a result, temperature during FSVB is higher than that during FSB. With increasing the brazing temperature, the flowability of the filler improves and filler completely fills the space between the joining specimens. Accordingly, the probability of porosity formation decreases. Additionally, it has been found that the size for agglomerated IMCs decreases as input flow increases and IMCs distribute more homogeneously [21].

IMCs might be the initial sites for the formation of cracks and cracks might form along the interface of IMCs and the matrix. It has been noted that crack formation around large IMCs is easier than that around small IMCs. The thickening of IMCs would deteriorate the bonding strength of joints [22–24].

Another point in Fig. 4 is the interface between the braze matrix and the base specimens. It is observed that for FSB-ed specimens, the interfacial boundaries at some regions are not coherent and discontinuity is observed in these regions, while for FSVB-ed specimens, the interfaces are coherent and continuous. The result suggested that vibration was able to disrupt layered IMC because IMC is easy to disrupt compared with the base metal [25]. Worth mentioning is that micro-bubbles are generated inside the molten filler during FSB and FSVB. During the collapse of the cavitation bubbles, the surface energy and kinetic energy of liquid are converted into heat and chemical energy. Local high temperatures aside from the pressure can be generated in this procedure. These effects provide a special local environment for IMC layer disruption and various novel chemical reactions [26–28]. The presence

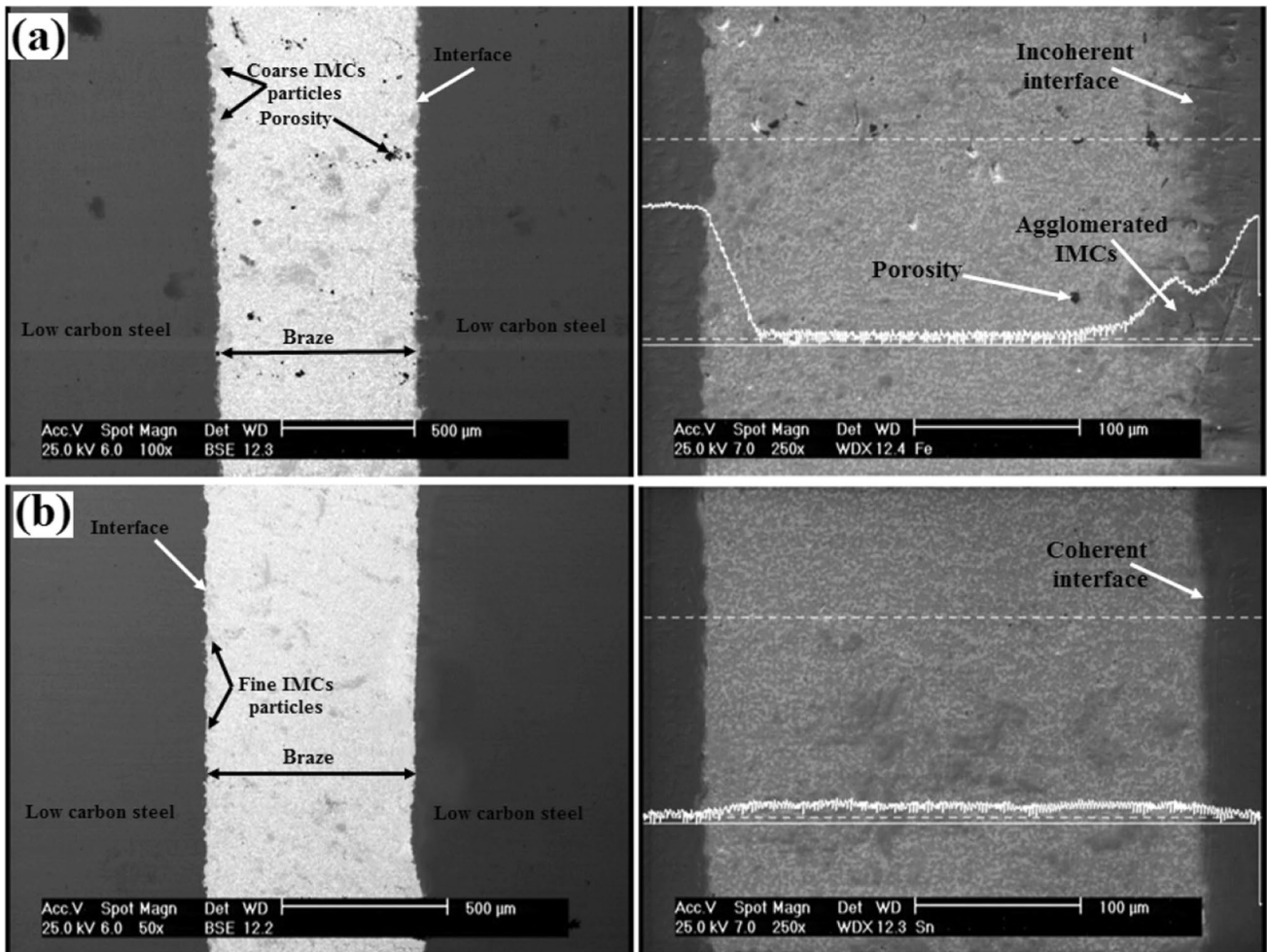


Fig. 4 Cross-section macrostructure of joints made by **a** FSB and **b** FSVB (rotation speed 1100 rpm, traverse speed 75 mm/min, and vibration frequency 25 Hz)

of vibration enhances the effects. The higher temperature during FSVB brings the possibility for higher diffusion of elements and as a result, a continuous interface is observed for FSVB-ed specimen.

The temperature in the joint region during FSVB is higher than that during FSB. Temperature variations versus time for a constant point of fixture recorded during FSB and FSVB processes are displayed in Fig. 5. According to Fig. 5, the temperature for both processes initially increases and then decreases. The first step relates to the time that the shoulder approaches the fixed point and the second step relates to the time that the shoulder gets away from the fixed point. For both processes, the maximum temperatures are higher than 200 °C (the melting point of filler is 187 °C), although the maximum temperature for FSVB is higher than that for FSB. This was related to more intensified friction when the joining specimens were vibrated during FSVB.

The EDS analysis results in Figs. 6 and 7 show the distribution of different elements for joints made by FSB and

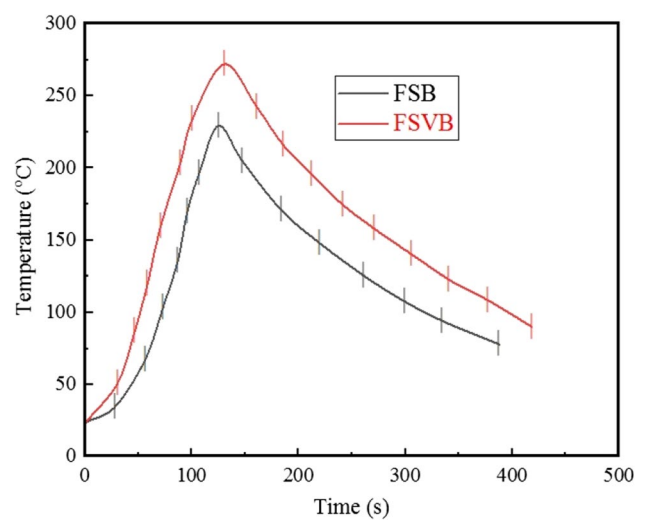


Fig. 5 Temperature history of a constant point of fixture relating to FSB and FSVB processes (rotation speed 1100 rpm, traverse speed 75 mm/min, and vibration frequency 25 Hz)

FSVB processes, respectively. According to these figures, Sn and Pb elements are observed massively in the joint regions, and Fe element is present in the joining specimens.

Si element is observed both in the joint region and in the joining specimens. Si in the joint region stems from SiC particles added to reinforce the joint. It comes from Figs. 6

Fig. 6 EDS maps showing the distribution of different elements in the joint made by FSB

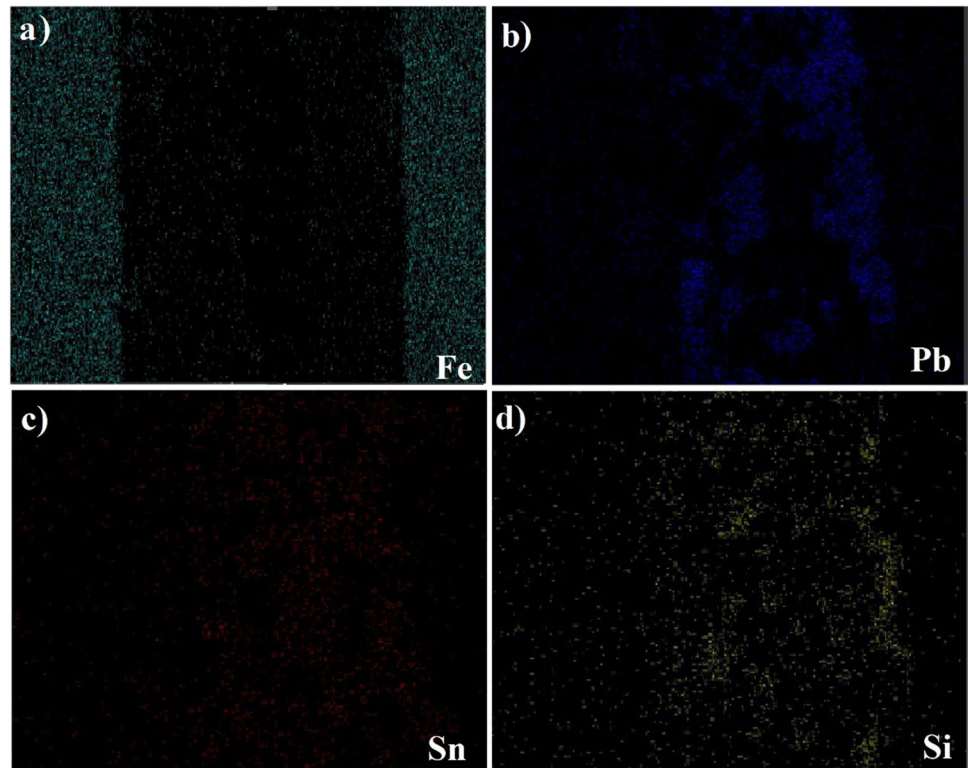
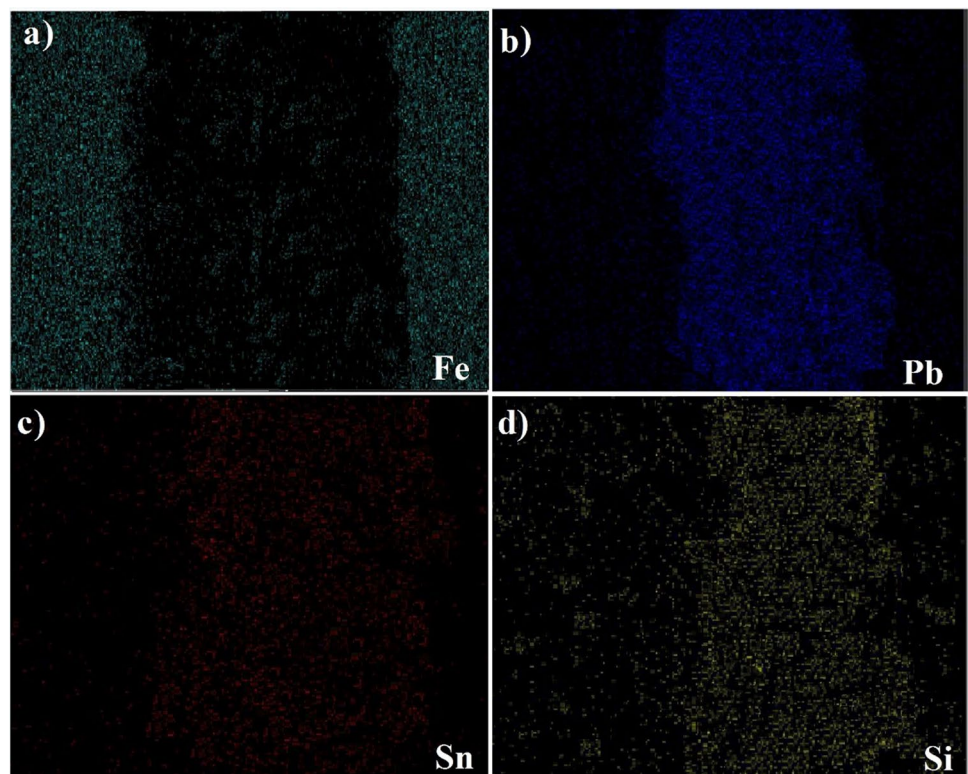


Fig. 7 EDS maps showing the distribution of different elements in the joint made by FSVB



and 7 that the Si distribution in the joint made by FSVB is more homogenous than that in the joint made by FSB. The authors believe that vibration results in higher deformation of filler material in the joint zone and the materials are stirred more. As a result, a more homogenous distribution of SiC particles is obtained. Bagheri et al. [29] through simulation of FSW analyzed the effect of vibration during FSW and found that the strain rate for joints produced by friction stir vibration welding (FSVW) was higher than that for joints fabricated by the conventional FSW process; additionally, the flow velocity measurements around the weld position for the former samples were higher in comparison to those for the latter samples.

There are two fundamental factors that control the joint strength, namely the intimate contact between joining interfaces and interfacial microstructure, especially the generation of IMCs. The poor wettability in FSB generally results from the poor mechanical effect on disrupting oxide film on steel surface rather than the absence of eutectic reaction [25]. SEM image of brazing for both FSB-ed specimen and FSVB-ed specimen as well as their chemical composition analysis by EDS without adding the reinforcing particles is presented in Fig. 8. Based on the phase diagram of Sn–Pb alloy [30–33], the alloy after solidification consists of a primary β (Sn-rich) phase and a eutectic mixture consisted of nearly pure lead (α) and nearly pure tin (β). α and β phases are observed as dark and light layers, respectively. As vibration is used during the FSB process, the development of high

pressure and temperature enhances the wettability between base alloy and filler material and, consequently, improves the thermally activated diffusion process. Therefore, the metallurgical reaction is drastically accelerated by mechanical vibration. After the FSVB process, the β -Sn phases became finer and smaller in size and are seemed more globular in shape. In addition, their homogeneity and even distribution increase during the FSVB process.

Figure 9 presents the LOM (light optical microscopy) images of the braze microstructures for both FSB and FSVB conditions. It indicates that grains in the joint zone under the FSVB process are smaller than those fabricated under the conventional FSB process. It can be associated with an increase in the nucleation sites which reduce the as-cast grain size during the FSVB process. Vibration led to a more homogenous structure as well as more turbulency which caused waves on the surfaces of the mold. Kocatepe [34] reported that these waves separate the primary nuclei nucleated on the surfaces of the mold. Thus, a collision happens among the nuclei and this leads to a uniform heat transfer mechanism. This process increases the nucleation rate and results in grain size reduction. It is concluded that the use of vibration enhances the fragmentation of the aggregated clusters and increases the flowability. The flow-ability indicates the ability of the plasticized material to move freely in different directions and to be mixed fairly.

It is worth mentioning that the nanoparticles because of their high surface area are prone to agglomerate to cut down

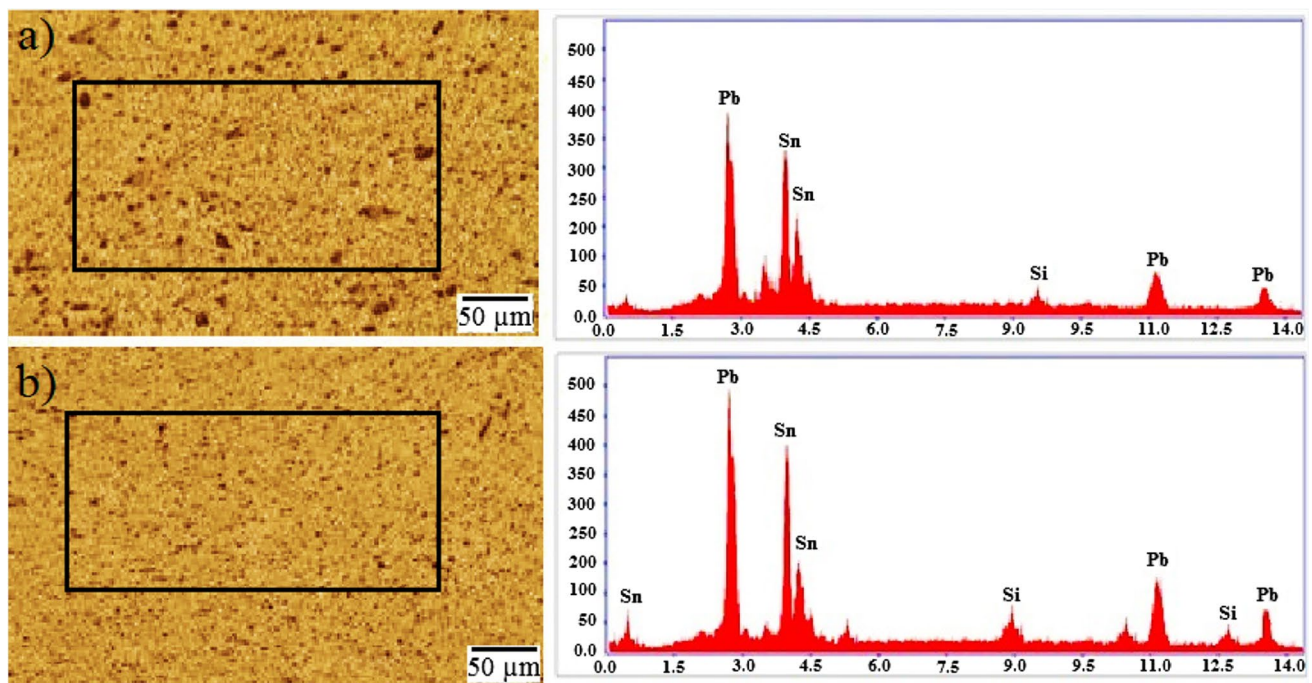
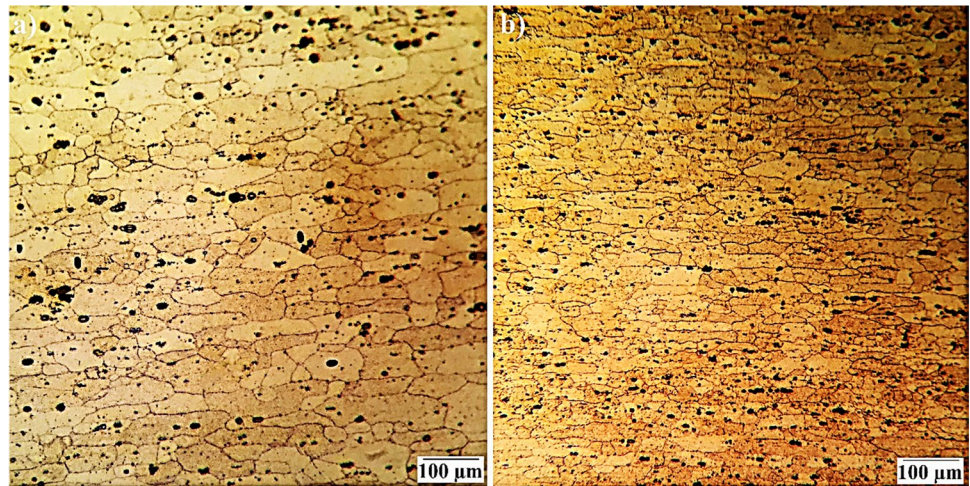


Fig. 8 SEM images of braze regions and chemical composition analyses of the selected areas by SEM–EDS for both **a** FSB and **b** FSVB (rectangle areas indicate the areas used for EDS analyses)

Fig. 9 Microstructures of braze regions relating to various brazing conditions. **a** FSB and **b** FSVB (rotation speed 1100 rpm, traverse speed 75 mm/min, and vibration frequency 25 Hz)

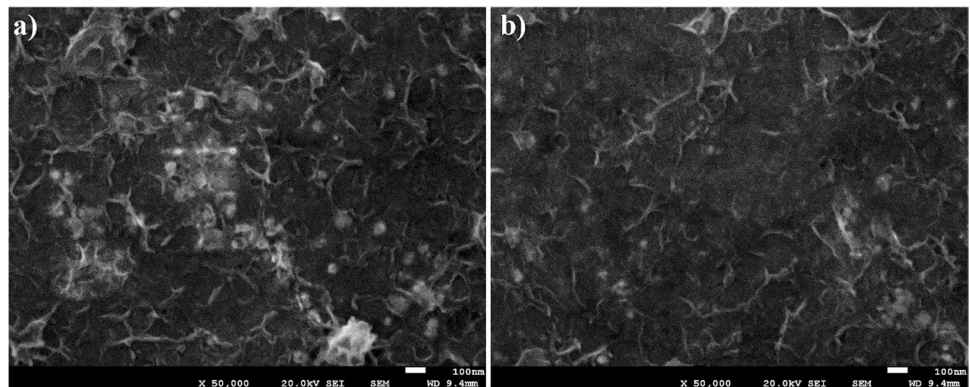


their overall energy [35]. This phenomenon arouses pores in the matrix and increases inter-particle spacing and as a result, reduces the strengthening of jointed samples. The SEM image of reinforcing particle distribution during both FSB and FSVB processes is shown in Fig. 10. From SEM analyses, it is observed that the distribution of reinforcing particles improves during the FSVB process compared to the FSB process. Second-phase particles hamper the grain growth and decrease the coarsening of the matrix pattern through pinning the motion of grain boundaries (Zener pinning effect) [36]. Regarding the SiC particles, they also increase the number of dislocations because of the coefficient of thermal expansion mismatch between the matrix and the reinforcement. Additionally, the SiC particles impede the microcrack propagation by inducing large differences in the elastic behavior between the matrix and the particle. Therefore, for FSVB-ed specimens which contain SiC particles with lower size and interparticle spacing, higher strength is predicted compared to FSB-ed specimens.

Shear test results of brazed samples for both joining conditions (FSB and FSVB) are depicted in Fig. 11. The actual fracture performance is decided by the relationship between

the stress distribution and mechanical properties [37]. Based on Fig. 11, the shear strength of brazed samples by FSVB is higher than that of the brazed samples by FSB. This may be associated with the smaller grain size and also higher homogeneity of particles as mentioned in the microstructural evolution section (Figs. 9 and 10). Based on the Hall–Petch relationship ($\sigma = \sigma_0 + kd^{-\frac{1}{2}}$) [38], strength (σ) improves as grain size (d) reduces. By decreasing the grain size, the volume fraction of grain boundaries improves. Grain boundaries hinder dislocations mobility and as a result, improve the strength of materials. The vibration of joining specimens during FSB leads to more homogenous intermixing of melt filler metal between the adjoining specimens and better adhesion of solidified melt to adjoining specimens is obtained. In this regard, interfacial boundary strength enhances. This increases the shear strength of brazed specimens made by the FSVB compared to the specimens fabricated by the FSB method. The presence of cavities and lack of diffusion in brazing metal under the FSB process is another reason for their low strength. Cavities lead to stress concentration and fracture occurs at low shear force values [38].

Fig. 10 SEM analyses of the distribution of reinforcing particles in the braze regions for **a** FSB and **b** FSVB (rotation speed 1100 rpm, traverse speed 75 mm/min, and vibration frequency 25 Hz)



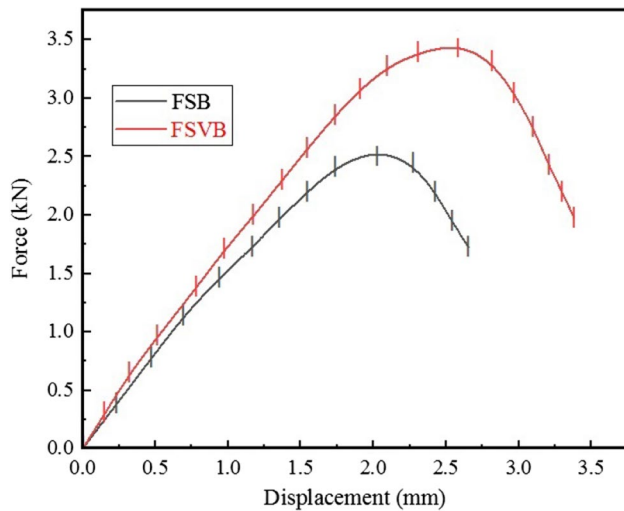


Fig. 11 Shear test results for samples brazed by FSB and FSVB (rotation speed 1100 rpm, traverse speed 75 mm/min, and vibration frequency 25 Hz)

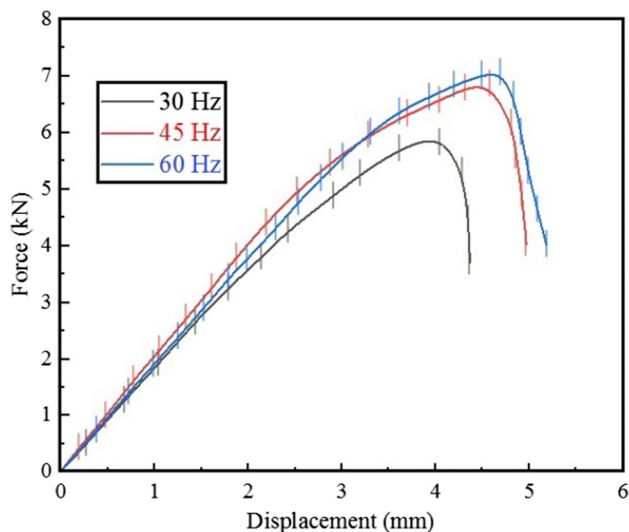


Fig. 12 Shear test results of brazed specimens under different vibration frequencies

3.2 Effect of vibration frequency

Shear test results for brazed specimens processed at various vibration frequencies, namely 30, 45, and 60 Hz, and SiC nanoparticles incorporated in the braze microstructure are presented in Fig. 12. The results indicate that the shear strength of brazed samples improves as vibration frequency improves. It has been well-known that the second-phase particles distributed in a ductile matrix are a typical source of alloy strengthening [39]. Particles intersect slip planes in a random fashion and a gliding dislocation must either

cut through the particles or penetrate the array of particles by bowing between the obstacles [40]. For both conditions, more force should be applied to move the dislocations. In addition, one significant result from Fig. 12 is the minor improvement of strength at high values of frequency. This shows that with an oscillation frequency of about 45 cycles/s, the highest strength and also ductility values are achieved and they do not vary remarkably as vibration frequency rises. It can be associated with the relation between strain and dislocation production. It has been reported by previous studies that the relation between the strain and dislocation production is not linear during work hardening and it follows a power-law relation [41]. That is, there is rapid improvement in dislocation production at low values of strain while this increment reduces at high values of strain.

Figure 13 indicates the grain size variation of the brazed samples under various vibration frequencies. The grain size is reduced as vibration is increased. As vibration improves, besides the stirring and traversing movement of the brazing tool, the material deformation increases. Since there is a direct relationship between material deformation (or strain) and the density of dislocations [42], so a quick multiplication of dislocations and a rapid increase in dislocation density happen by increasing strain. It finally leads to finer grains in the brazed samples. It is worth mentioning that no significant change in the grain size is shown when frequency increases from 45 to 60 Hz due to the power law relation between strain and dislocation density mentioned in the previous section.

By increasing the vibration frequency during FSVB, the distribution of second-phase particles changes and it becomes more homogenous. TEM images of braze microstructures relating to the FSVB-ed specimens at different vibration frequencies and contained SiC particles are displayed in Fig. 14. It is seen that the particles are distributed more homogeneously and less agglomeration occurs as vibration frequency enhances. The material in the brazed zone experiences more deformation as vibration frequency improves. The presence of mechanical vibration leads to the breakdown of agglomerated reinforcing particles and increases the homogeneity of SiC particle distribution. The thermal expansion mismatch between the base metal and filler material can generate residual stresses in the joints during cooling after soldering. The stress relaxation or creep deformation of the brazed specimen is expected to mitigate the mismatch of the thermal expansion coefficients between filler and the base metal [43].

The severe plastic deformation and temperature generated during brazing have a considerable effect on the formation of the intermetallic phase. The interfacial IMC layer thickness relating to various vibration frequency values for both top and bottom interfaces was measured using Eq. 1, and the results are presented in Fig. 15. It is seen that the thickness

Fig. 13 The grain size variation in the brazed samples under various vibration frequencies. **a** 30 Hz, **b** 45 Hz, and **c** 60 Hz

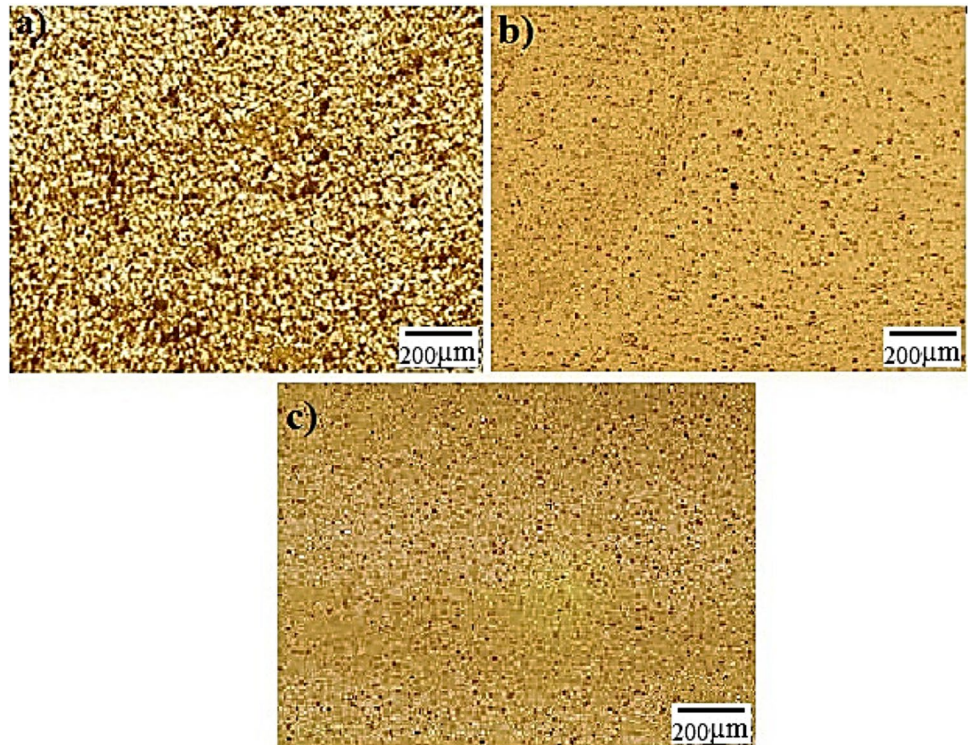
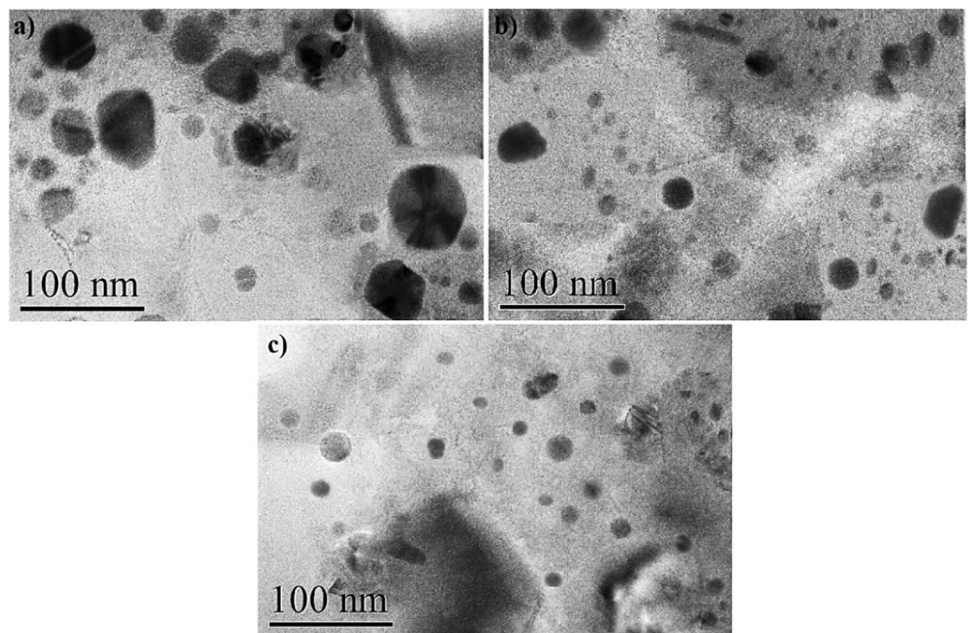


Fig. 14 TEM analysis of SiC particles relating to brazed specimens at different vibration frequencies. **a** 30 Hz, **b** 45 Hz, and **c** 60 Hz



of IMCs in joints made by conventional FSB is the highest value and for the joints made by FSVB process with 60-Hz vibration frequency, it is the lowest. This layer performs as a barrier and resists against the indenter movement during hardness testing and raises the hardness. However, the mechanical vibration breaks the IMC layer into small particles and distributes them evenly in the joint zone. The difference in thickness between the top and bottom interfacial

IMC layers is because of placing the vibration plate under the workpiece, in which the effect of vibration frequency is higher than the top interface. However, this discrepancy has been found to decrease with increasing vibration frequency.

As vibration frequency increases, due to severe contact between tool and base metal, temperature increases [43], and the melt, between the adjoining specimens, flows more easily. More fluidity of melt, due to higher temperature, causes

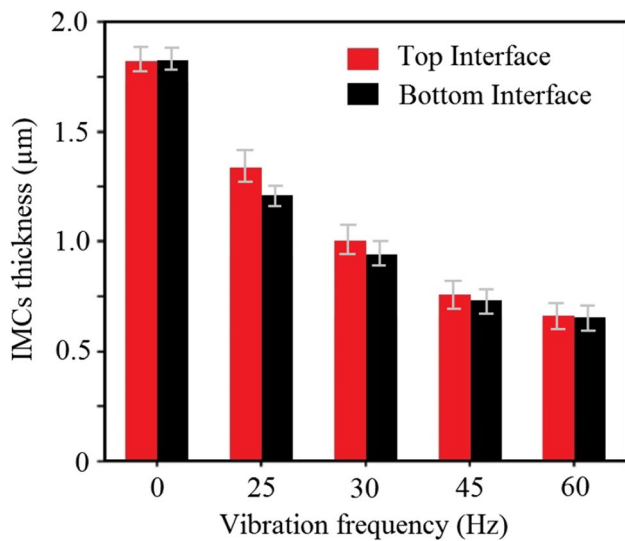


Fig. 15 Interfacial IMC layers thickness for various brazing conditions. FSB and FSVB with different vibration frequencies (25, 30, 45, and 60 Hz)

the more homogenous distribution of SiC nanoparticles. The degree of strengthening based on second-phase particles is dependent on different parameters including the volume fraction, the shape of particles, the particle diameter, and also the interparticle spacing of particles [38]. According to the Orowan theory [38], strengthening presented by second-phase particles is given by the following equation:

$$\Delta\sigma = \frac{\alpha Gb}{\lambda} \ln \quad (2)$$

where:

α : constant.

G : shear modulus.

b : Burgers vector.

r : radius of spherical particles.

λ : interparticle spacing and a simple expression for it is:

$$\lambda = \frac{4(1-f)r}{3f} \quad (3)$$

where f is the volume fraction of spherical particles of radius r .

By increasing the vibration frequency, homogeneity of SiC particle distribution improves and their agglomeration reduces. Less agglomeration of SiC particles means less r value. Regarding the constant volume fraction of particles, λ decreases as r decreases. So, a more homogenous distribution of SiC particles results in less r and λ values, and according to Eq. 2, strengthening because of the presence of second-phase particles improves more and higher strengthening is obtained [43].

Table 3 Hardness values for base material and braze metal for different brazing conditions

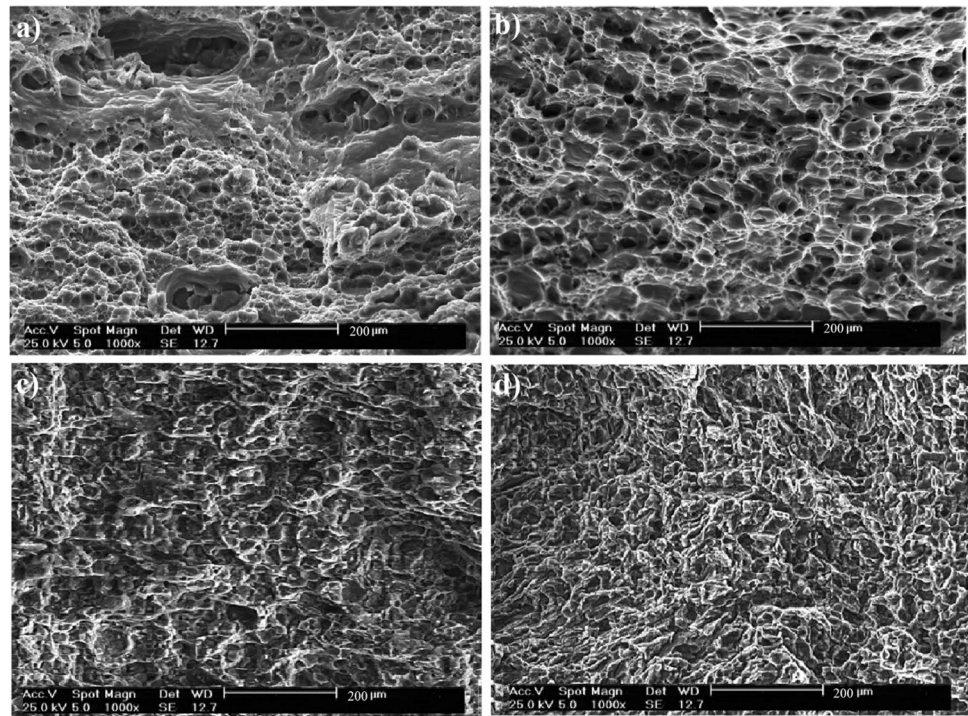
	Hardness (HV)
FSB + Powder	16.5 ± 2
FSVB-30 Hz + Powder	23.1 ± 2
FSVB-45 Hz + Powder	27.5 ± 2
FSVB-60 Hz + Powder	28.2 ± 2
Base	125 ± 2

Hardness test measurement results for various brazed specimens processed by different vibration frequencies are displayed in Table 3. The hardness values relate to the brazing metal between the adjoining specimens. Based on data in Table 3, the hardness value for the brazed sample improves as vibration frequency increases. Hardness which is considered as the resistance of a substance to localized plastic deformation depends greatly on dislocations movement [44]. Variables that reduce the motion of dislocations increase the hardness. The presence of second-phase particles restricts the mobility of dislocations and more force should be applied to move them [40]. Additionally, according to Eq. 2, the resistance of second-phase particles to the movement of dislocations increases as particles are distributed more homogeneously (lower r and λ values). It was observed in Fig. 15 that the SiC particles distributed more homogeneously as vibration frequency increased. The results obtained are in good agreement with the previous studies [2, 45], in which enhanced uniformity of the structure of β -Sn phase and the dispersion of eutectic phase improved the resistance against dislocation and resulted in a higher hardness profile.

3.3 Fractured surface analysis

Figure 16 indicates the fractured image of the joint zone for specimens made by FSB and FSVB while both specimens include reinforcing particles in the joint zone. The fundamental point of these images is the presence of dimples. Dimples usually form because of dislocation intersection, and they indicate a ductile fracture in samples [46–48]. In the first step of the deformation process, the dislocations are able to slip, climb, and cross-slip. Frank–Read sources and multiplication by the double-cross slip have been considered as some mechanisms for dislocation production and they can be activated through the improvement of deformation. However, by an increment of dislocations density, the interaction between dislocations leads to the generation of some dislocation locks that impede the higher slip of dislocations. In this condition, a higher improvement in the implemented force results in the generation of voids at the lock sites. Voids grow and dimples form and finally a ductile fracture occurs. The fracture surfaces of joints made by

Fig. 16 Fracture features of joints made by various brazing conditions. **a** FSB, **b** FSVB (30 Hz), **c** FSVB (45 Hz), and **d** FSVB (60 Hz)



the FSB method show coarse dimples as opposed to a large number of fine dimples in the fracture surface of joints made by FSVB. These can be associated with the role of grain size and also the distribution of reinforcing particles during the brazing process with various conditions. By decreasing the grain size, the mobility of dislocations and accretion of voids reduce, and consequently, the generation and growth of large voids reduce. On the other side, the site for void formation decreases as the grain size and agglomerated particles size decrease by an increment of vibration frequency. This is validated by the obtained brazed matrix hardness as shown in Table 3 and grain size distribution as observed in Fig. 13.

4 Conclusions

FSB as a joining method is based on metallurgical reaction instead of plastic flow. Different trials have been carried out to improve the mechanical properties of joints made by FSB. In the current research, a modified version of the FSB process, entitled FSVB, is presented. In this method, joining specimens are vibrated mechanically during FSB, in a direction normal to tool transverse direction. Steel plates were joined by FSB and FSVB methods while %67wt Sn-%33wt Pb alloy was applied as brazing material and SiC particles were incorporated in the braze microstructure. Microstructure and mechanical properties of brazed samples at different brazing conditions were compared. It was concluded that:

1. FSVB provides higher joint strength, hardness, and finer grain size than those when using FSB.
2. Vibration in FSVB increases the fluidity of molten filler and as consequence, it enhances the homogeneity of strengthening particles distribution.
3. The strength and hardness of joints made by FSVB enhance as vibration frequency increases, while the grain size and the thickness of IMCs in the joint decrease.
4. FSVB as a new brazing method, which results in joints with proper mechanical properties, is proposed to welding communities and it is recommended for application in industries.

References

1. Abtey M, Selvaduray G (2000) Lead-free solders in microelectronics. *Mater Sci Eng R Rep* 27:95–141
2. Tan AT, Tan AW, Yusof F (2017) Evolution of microstructure and mechanical properties of Cu/SAC305/Cu solder joints under the influence of low ultrasonic power. *J Alloy Comp* 25:188–197
3. Mohd Salleh MAA, McDonald SD, Gourlay CM, Yasuda H, Nogita K (2016) Suppression of Cu₆Sn₅ in TiO₂ reinforced solder joints after multiple reflow cycles. *Mater Des* 108:418–428
4. Ma ZL, Belyakov SA, Gourlay CM (2016) Effects of cobalt on the nucleation and grain refinement of Sn-3Ag-0.5Cu solders. *J Alloy Comp* 682(2016):326–337

5. Jing Y, Gao X, Su D, Zhao C, Jiang J (2018) The effects of Zr level in Ti-Zr-Cu-Ni brazing fillers for brazing Ti-6Al-4V. *J Manuf Process* 31:124–130
6. Sharma A, Lee SJ, Choi DY, Jung JP (2017) Effect of brazing current and speed on the bead characteristics, microstructure and mechanical properties of the arc brazed galvanized steel sheets. *J Mater Process Tech* 249:212–220
7. Zhang G, Su W, Zhang J, Wei Z (2011) Friction stir brazing: a novel process for fabricating Al/steel layered composite and for dissimilar joining of Al to steel. *Metal Mater Trans A* 42A:2850–2861
8. Mishra RS, Ma ZY (2005) Friction stir welding and processing. *Mater Sci Eng R* 50:1–78
9. Jafari M, Abbasi M, Poursina D, Gheysarian A, Bagheri B (2017) Microstructure and mechanical properties of friction stir welded dissimilar steel-copper joints. *J Mech Sci Tech* 31:1135–1142
10. Abbasi M, Bagheri B, Dadaei M, Omidvar H, Rezaei M (2015) The effect of FSP on mechanical, tribological and corrosion behavior of composite layer developed on magnesium AZ91 alloy surface. *J Adv Manuf Tech* 77:2051–2058
11. Yang JG, Wu JW, Fang HY (2003) Effects of Al₂O₃ particulates on the thickness of reaction layer of Al₂O₃ joints brazed with Al₂O₃-particulate-contained composite filler materials. *J Mater Sci Technol* 19:509–510
12. Chuang TH, Wu MW, Chang SY, Ping SF, Tsao LC (2011) Strengthening mechanism of nano-Al₂O₃ particles reinforced Sn_{3.5}Ag_{0.5}Cu lead-free solder. *J Mater Sci Mater Electron* 22:1021–1027
13. Javadi MJ, Fazel-Najafabadi M (2014) Effect of friction stir brazing parameters on microstructure and mechanical properties of dissimilar alloys joint. *Indi J Sci Res* 2:615–622
14. Huang G, Feng X, Shen Y, Zheng Q, Zhao P (2016) Friction stir brazing of 6061 aluminum alloy and H22 brass: evaluation of microstructure, mechanical and fracture behavior. *Mater Des* 99:403–411
15. Wei Cu, Shuqi L, Jiuchun Y, Xing Zh (2018) Microstructure and mechanical performance of composite joints of sapphire by ultrasonic-assisted brazing. *J Mater Process Tech* 257:1–6
16. Chen X, Xie R, Lai Zh, Liu L, Yan J, Zou G (2017) Interfacial structure and formation mechanism of ultrasonic-assisted brazed joint of SiC ceramics with Al-12Si Filler Metals in Air. *J Mater Sci Tech* 33:492–498
17. Vianco P, Hosking F, Rejent J (1996) Ultrasonic soldering for structural and electronic applications. *Weld J* 75:343–355
18. Huang G, Huang J, Zhang M, Mu D, Zhou G, Xu X (2018) Fundamental aspects of ultrasonic assisted induction brazing of diamond onto 1045 steel. *J Mater Process Tech* 260:123–136
19. Xu G, Leng X, Jiang H, Xiu Z, Yan J (2020) Microstructure and strength of ultrasonic-assisted brazed joints of Si₃N₄/6061Al composites. *J Manuf Process* 54:89–98
20. Zhang Ch, Ji H, Xu H, Liang M, Huang J, Pei Sh, Li M (2020) Interfacial microstructure and mechanical properties of ultrasonic-assisted brazing joints between Ti-6Al-4V and ZrO₂. *Ceramic Int* 46:7733–7740
21. Davies SH (2001) *Theory of solidification*. Cambridge University Press, New York
22. Li C, Si XQ, Dai XY (2019) Understanding the effect of surface machining on the YSZ/Ti6Al4V joint via image based modelling. *Sci Rep* 9(1):1–13
23. Abbasi M, Bagheri B, Abdollahzadeh A, Moghaddam AO (2021) A different attempt to improve the formability of aluminum tailor welded blanks (TWB) produced by the FSW. *Int J Mater Form* 14:1189–1208
24. Bagheri B, Abbasi M, Abdollahzadeh A, Kokabi AH (2020) A comparative study between friction stir processing and friction stir vibration processing to develop magnesium surface nanocomposite. *J Min Metal Mater* 27:1133–1146
25. Bagheri B, Abdollahzadeh A, Abbasi M, Kokabi AH (2020) Numerical analysis of vibration effect on friction stir welding by smoothed particle hydrodynamics (SPH). *J Adv Manuf Technol* 110:209–228
26. Zhang G, Yang X, Zhu D, Zhang L (2020) Cladding thick Al plate onto strong steel substrate using a novel process of multilayer-friction stir brazing (ML-FSB). *Mater Des* 185:108232
27. Brujan EA, Ikeda T, Matsumoto Y (2008) On the pressure of cavitation bubbles. *Exp Therm Fluid Sci* 32(5):1188–1191
28. Wagterveld RM, Boels L, Mayer MJ, Witkamp GJ (2011) Visualization of acoustic cavitation effects on suspended calcite crystals. *Ultrason Sonochem* 18(1):216–225
29. Bagheri B, Abbasi M, Hamzeloo R (2020) The investigation into vibration effect on microstructure and mechanical characteristics of friction stir spot vibration welded aluminum: Simulation and experiment. *Proc Ins Mech Eng: Part C J Mech Eng Sci* 234(9):1809–1822
30. Massalski TB (1990) *Binary alloy phase diagrams*, 2nd edn. ASM International, USA
31. Shen YL, Abell KCR, Garrett SE (2004) Effects of grain boundary sliding on microstructural evolution and damage accumulation in tin-lead alloy. *Int J Damag Mechanic* 13:225–240
32. Cui W, Li SH, Yan J, He J, Liu Y (2015) Ultrasonic-assisted brazing of sapphire with high strength Al-4.5Cu-1.5Mg alloy. *Ceramic Int* 41:8014–8022
33. Gencalp S, Saklakoglu N (2012) Effects of low-frequency mechanical vibration and casting temperature on microstructure of semisolid AlSi₈Cu₃Fe alloy. *Arab J Sci Eng* 37:2255–2267
34. Kocatepe K (2007) Effect of low frequency vibration on porosity of LM25 and LM6 alloys. *Mater Des* 28:1767–1775
35. Bagheri B, Abbasi M, Dadaei M (2020) Mechanical behavior and microstructure of AA6061-T6 joints made by friction stir vibration welding. *J Mater Eng Perform* 29:1165–1175
36. Porter DA, Easterling KE, Sherif M (2009) *Phase transformation in metals and alloys*, 3rd edn. CRC Press, New York, pp 156–165
37. Yang ZW, Zhang LX, Chen YC, Qi JL, He P, Feng JC (2013) Interlayer design to control interfacial microstructure and improve mechanical properties of active brazed Invar/SiO₂-BN joint. *Mater Sci Eng A* 575:199–205
38. Zhao YX, Wang MR, Cao J, Song XG, Tang DY, Feng JC (2015) Brazing TC4 alloy to Si₃N₄ ceramic using nano-Si₃N₄ reinforced Ag-Cu composite filler. *Mater Des* 76:40–46
39. Dai X, Cao J, Chen Z, Song X, Feng J (2016) Effect of holding time on microstructure and mechanical properties of SiC/SiC joints brazed by Ag-Cu-Ti+B₄C composite filler. *Mater Character* 118:294–301
40. Dieter GE (1988) *Mechanical metallurgy*. McGraw-Hill Book Company, Singapore
41. Bulatov V, Cai W (2006) *Computer simulations of dislocations*. Oxford Materials, Oxford, pp 243–249
42. Callister WD (1994) *Materials science and engineering: an introduction*. John Wiley & Sons Inc, New York
43. Hertzberg RW (1989) *Deformation and fracture mechanics of engineering materials*. John Wiley & Sons Inc, New York
44. Abdollahzadeh A, Bagheri B, Abbasi M, Kokabi AH, Moghaddam AO (2021) Comparison of the weldability of AA6061-T6 joint under different friction stir welding conditions. *J Mater Eng Perform* 30:1110–1127
45. Tan AT, Tan AW, Yusof F (2016) Influence of high-power-low-frequency ultrasonic vibration time on the microstructure and mechanical properties of lead-free solder joints. *J Mater Process Technol* 238:8–14
46. Bagheri B, Abbasi M, Abdollahzadeh A, Mirsalehi SE (2020) The effect of second phase particle size and presence of vibration

- on AZ91/SiC surface composite layer produced by FSP. *Trans Nonferrous Metal Soc Chin* 30:905–916
47. Abbasi M, Givi M, Bagheri B (2019) Application of vibration to enhance efficiency of friction stir processing. *Trans Nonferrous Metal Soc Chin* 29:393–1400
 48. Bagheri B, Abbasi M (2020) Development of AZ91/SiC surface composite by FSP: effect of vibration and process parameters on microstructure and mechanical characteristics. *Adv Manuf* 8:82–96

Publisher's note Springer Nature remains neutral with regard to jurisdictional claims in published maps and institutional affiliations.